

THE CLUSTERING OF FAINT GALAXIES

G. EFSTATHIOU,¹ G. BERNSTEIN,^{2,3} N. KATZ,^{1,4} J. A. TYSON,^{2,3} AND P. GUHATHAKURTA^{5,3}

Received 1991 April 8; accepted 1991 July 29

ABSTRACT

Deep images of the sky have revealed a population of faint blue objects that may be protogalaxies at redshifts $z \gtrsim 1$. In this letter we show that these faint galaxies are surprisingly weakly clustered. There are several possible explanations of this result: (1) the majority of the faint blue galaxies belong to a new population that is weakly clustered and intrinsically faint at the present epoch; (2) galaxy clustering evolves much more rapidly than expected in simple models of gravitational instability; or (3) the geometry of the universe differs significantly from the Einstein–de Sitter model.

Subject headings: cosmology — galaxies: clustering — galaxies: formation

1. INTRODUCTION

The possibility that the faint blue galaxies found in deep CCD images (Tyson 1988; Cowie et al. 1988) may be ordinary galaxies at an early stage of evolution has excited much interest. The arguments in favour of this idea are indirect, however, and it is possible that the faint population represents a new class of object. A hint of the latter follows from the high space density implied by the faint counts which exceeds the space density expected of ordinary luminous galaxies (Cowie 1989; Koo 1991).

As a further test of the nature of the faint galaxies, we have measured their two-point angular correlation function, $w(\theta)$, where

$$\delta P = \mathcal{N}^2 [1 + w(\theta)] \delta\Omega_1 \delta\Omega_2, \quad (1)$$

is the joint probability of finding galaxies in the solid angle elements $\delta\Omega_1$ and $\delta\Omega_2$ separated by angle θ and \mathcal{N} is the mean surface density of galaxies. An independent analysis of the clustering of faint galaxies is described by Windhorst & Neuschaefer (1991) and Neuschaefer, Windhorst, & Dressler (1992).

2. OBSERVED CORRELATIONS

We have analyzed the 12 deep CCD fields surveyed by Tyson & Seitzer (1988), (hereafter TS12) with a total area of 107 arcmin² in each of B_J , R , and I filters. In addition, we have used a deep (5100 s effective exposure) large-format CCD B_J image, taken on the KPNO 4 m telescope, covering 49 arcmin² in the SA68 field. Comparably deep U data on three of the TS12 fields (Guhathakurta, Tyson, & Majewski 1990) covering about 27 arcmin² have also been analyzed.

The FOCAS automated detection software (Jarvis & Tyson 1981; Valdes 1982) has been used to reduce each CCD image to an object catalog from which we extract the centroid positions of all objects in a selected magnitude range. We deter-

mine the angular correlation function using the estimator

$$w(\theta) = \frac{N_{dd}(\theta)}{N_{dr}(\theta)} \frac{2n_r}{(n_d - 1)} - 1, \quad (2)$$

where n_d and n_r in turn denote the number of data points and of a set of uncorrelated random points laid down in the field. The quantities N_{dd} and N_{dr} are the number of (distinct) data-data and data-random pairs, respectively, with the desired angular separation. For the SA68 field we have also applied the estimator

$$w(\theta) = \frac{\langle N_i N_j \rangle}{\langle N_i \rangle \langle N_j \rangle} - 1, \quad (3)$$

where N_i and N_j are the counts in cells i and j , and the angular brackets denote an average over pairs of cells separated by an angle $\theta \pm \delta\theta$. Areas around bright stars and galaxies, adding up to roughly 6% of the total area, are excluded from the analysis.

We have determined $w(\theta)$ using all objects with isophotal magnitude $24 < B_J < 26$. The correlation functions derived for the TS12 fields are combined with equal weight per field to compute a mean $w(\theta)$ and its standard deviation. The B_J angular correlation function for the TS12 fields is plotted in Figure 1a together with 1σ error bars. Angular correlation functions for SA68 are plotted in Figure 1b. For this field, the estimates derived from equation (2) (filled circles) show a linear trend with θ and become negative at $\theta \gtrsim 30''$. This behavior suggests a low-amplitude large-scale gradient in the galaxy density across the field. The estimates of $w(\theta)$ for this field derived from equation (3) (*open circles*) are very close to zero at large scales and are likely to be more reliable.

Within the above magnitude range, the catalogs are free of spurious (noise) images, and are nearly complete for objects with surface brightnesses above our detection threshold of $29 B_J$ mag arcsec⁻². Our results are insensitive to whether or not we include those objects morphologically classified by FOCAS as “stars” ($\sim 10\%$ of the total). We use all objects in the results presented here.

We have binned together all pairs with $15'' \lesssim \theta \lesssim 45''$ (shown by the horizontal line segments in Fig. 1). These values of θ are large enough to avoid problems of undercounting caused by the crowding of galaxy isophotes [see $w(\theta)$ for $\theta \lesssim 10''$ in Fig. 1] and yet are much smaller than the extent of the individual TS12 fields. Assuming $w(\theta) \propto \theta^{1-\gamma}$, $\gamma = 1.8$, the

¹ Department of Physics, Nuclear Physics Laboratory, Keble Road, Oxford, OX1 3RH, England.

² AT&T Bell Laboratories, 1D335, 600 Mountain Avenue, Murray Hill, NJ 07974.

³ Visiting Astronomers at NOAO operated by the Association of Universities for Research in Astronomy Inc., under contract with the National Science Foundation.

⁴ Department of Physics, MIT 6-207, Cambridge, MA 02139.

⁵ Institute for Advanced Study, School of Natural Sciences, Olden Lane, Princeton, NJ 08540.

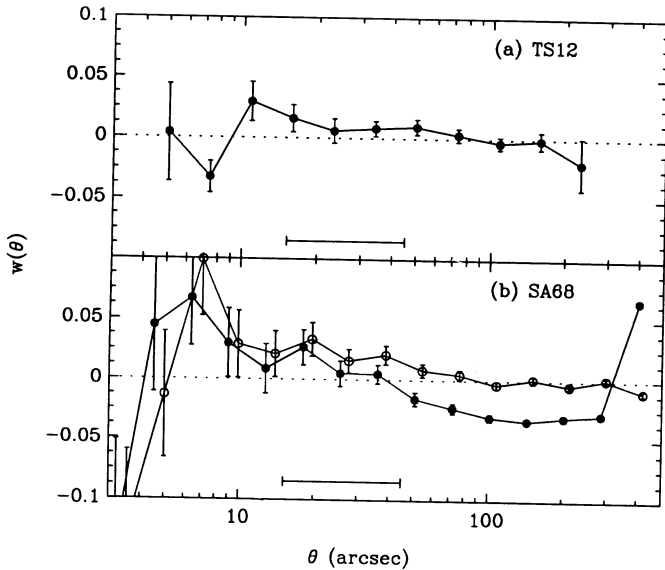


FIG. 1.—Angular correlation functions for faint galaxies in the magnitude range $24 < B_J < 26$. The solid symbols in Fig. 1a show the mean angular correlation function for the 12 fields TS12 and the error bars show the field-to-field fluctuations. Fig. 1b shows $w(\theta)$ for the SA68 field together with Poisson errors. The filled symbols in Fig. 1b show the direct estimate of $w(\theta)$ from eq. (2) and the open symbols show the ensemble-averaged estimate that corrects for large-scale gradients in the galaxy surface density (eq. [3]). The horizontal lines show the range of angular scales used to compute the values of $w(\theta)$ listed in Table 1.

effective value of θ in this broad bin is $\sim 30''$ (and is insensitive to γ). In the first row of Table 1, we list values of w in this broad bin, $w(30'')$, computed from equation (2) for the TS12 fields and equation (3) for SA68. The correlation function has also been evaluated using TS12 objects with $23 < R < 25$ and for those with $22 < I < 24$, and from the three U fields for objects with $23.5 < U < 25.5$. These magnitude ranges are chosen to be roughly centred on the average R , I , and U magnitudes of galaxies in the range $24 < B_J < 26$ (Tyson 1988; Guhathakurta et al. 1990). A little over half the TS12 B_J galaxies also belong to the R group, while nearly three quarters of the R sample are in the B_J sample. In order to improve the reliability of the somewhat noisier I -selected sample, we include only those I objects that are also detected in the R band ($R \lesssim 27$) or the B_J band ($B_J \lesssim 28$). In addition, the TS12 B_J sample has been divided according to $B_J - R$ color about the median value of 0.6 into the “ B_J red” and “ B_J blue” samples.

The second line in Table 1 lists the 1σ error in the mean of $w(30'')$. For the TS12 B_J , R , and I samples, these errors are estimated from the field-to-field variance and are comparable to or slightly larger (by up to 30%) than the Poisson error, $N_{dd}^{-1/2}$. We quote Poisson errors for SA68 and the three-field U sample. The numbers of objects in each sample used to calculate $w(\theta)$ are given in the last row of Table 1.

In B_J , $w(30'')$ for the SA68 field is clearly positive (see Fig. 1) and is higher than our estimate for the TS12 fields. The R and I samples also give positive values of $w(30'')$ with slightly larger uncertainties. We find no detectable correlations in the U sample. The R - and I -selected galaxies are clustered slightly more strongly than those in the TS12 B_J and U samples. The blue objects in the B_J sample appear to have a larger $w(30'')$ than the red ones but this effect is not statistically significant. The reality of these effects will be tested with a larger sample of galaxies in a future paper, where we plan to study $w(\theta)$ as a function of apparent magnitude and color.

In estimating $w(\theta)$ we have used the actual object count n_d on each field rather than the mean count $\langle n_d \rangle$ averaged over all fields. This avoids any spurious signals arising from field-to-field variations in seeing, noise levels, extinction, and magnitude scale, but causes the angular correlation function to be underestimated by

$$\sigma^2 = \frac{1}{\Omega^2} \iint w(\theta) d\Omega_1 d\Omega_2 \quad (4)$$

(Groth & Peebles 1977), where θ is the angle separating the solid angle elements $d\Omega_1$ and $d\Omega_2$ and the integrals in (4) are over the solid angle Ω of the field. If we assume a true angular correlation function $w^T(\theta) \propto \theta^{-0.8}$, we obtain $\sigma^2 = 0.53w^T(30'')$ for the TS12 fields, and $\sigma^2 = 0.27w^T(30'')$ for the SA68 field. This explains why the TS12 estimates of $w(\theta)$ are lower than those from the SA68 field. Combining the results in Table 1 and correcting for the finite field sizes gives our best estimate of 0.024 ± 0.004 for the galaxy-galaxy correlation function at $30''$ in the B_J band.

The field-to-field variance in the number counts should be equal to

$$\left\langle \frac{n_d - \langle n_d \rangle}{\langle n_d \rangle} \right\rangle^2 = \frac{1}{\langle n_d \rangle} + \sigma^2$$

in the absence of variations in extinction, etc., mentioned above. The TS12 fields⁶ give $\sigma^2 = 0.012 \pm 0.004$ for the B_J sample, which is in excellent agreement with equation (4) for a power-law correlation function with our “best-fit” amplitude of $w(30'') = 0.024$ and slope -0.8 .

3. EXPECTED CORRELATIONS

The two-point angular correlation function is related to its spatial analog $\zeta(r)$ by an integral equation (see § 56 in Peebles 1980). The spatial correlation function measured from nearby samples of galaxies is well approximated by a power law

⁶ Since the fields have slightly different areas Ω_i , we instead estimate the excess variance using

$$\sigma^2 = [\sum (n_i^2 - \mathcal{N}^2 \Omega_i^2)] / (\mathcal{N}^2 \sum \Omega_i^2) - (1/\mathcal{N}) (\sum \Omega_i) / (\sum \Omega_i^2),$$

where \mathcal{N} is the mean surface density averaged over all fields.

TABLE 1
OBSERVED GALAXY-GALAXY ANGULAR CORRELATION (UNCORRECTED)

PARAMETER	SA68	TS12					
	B_J	B_J	R	I	U	B_J red	B_J blue
$w(30'')$	0.022	0.009	0.014	0.020	-0.004	0.003	0.020
σ_w	0.006	0.006	0.007	0.006	0.010	0.010	0.009
N_{obj}	1570	3631	2731	2560	639	1571	1538

$\xi(r) = (r_0/r)^\gamma$ at $r \lesssim 10h^{-1}$ Mpc with $r_0 \approx 5.5h^{-1}$ Mpc and $\gamma \approx 1.8$ (where h is the Hubble constant H_0 in units of $100 \text{ km s}^{-1} \text{ Mpc}^{-1}$). For small angles ($\theta \ll 1$), the relation between $w(\theta)$ and $\xi(r)$ becomes

$$w(\theta) = \sqrt{\pi} \frac{\Gamma[(\gamma-1)/2]}{\Gamma(\gamma/2)} \frac{A}{\theta^{\gamma-1}} r_0^\gamma, \quad (5a)$$

$$A = \int_0^\infty g(z) \left(\frac{dN}{dz} \right)^2 dz / \left[\int_0^\infty \left(\frac{dN}{dz} \right) dz \right]^2,$$

where

$$g(z) = \left(\frac{dz}{dx} \right) x^{1-\gamma} F(x) (1+z)^{-(3+\epsilon-\gamma)},$$

$$\xi(r, z) = \left(\frac{r_0}{r} \right)^\gamma (1+z)^{-(3+\epsilon)}, \quad (5b)$$

and x is the coordinate distance at redshift z , dN/dz is the number of objects per unit redshift interval in the sample and the metric is

$$ds^2 = c^2 dt^2 - a^2 [dx^2/F(x)^2 + x^2 d\theta^2 + x^2 \sin^2 \theta d\phi^2],$$

where a is the cosmological scale factor (Peebles 1980). If the clustering pattern were fixed in comoving coordinates, then $\epsilon = \gamma - 3 \approx -1.2$; this should roughly describe the evolution of ξ in theories where galaxies are identified with peaks in the mass density field and hence are strongly clustered ab initio (Davis et al. 1985; Carlberg 1991). However, if galaxy clustering is dynamically bound and stable at small scales, then the clustering pattern will remain fixed in proper coordinates r and so $\epsilon \approx 0$ and $\epsilon = -1.2$ in evaluating equation (5) which should bracket the range expected in many models of galaxy formation and clustering.

To evaluate equations (5), we need to know the redshift distribution dN/dz of faint galaxies. At $B_J \sim 21-24$, the median redshift of field galaxies appears to be in the range 0.3-0.4 (Colless et al. 1990; Lilly, Cowie, & Gardner 1991) but very little is known about the redshift distribution of galaxies at $B_J > 24$. Guhathakurta et al. (1990) argue from the $U-B_J$ colors that less than $\sim 7\%$ of galaxies with $B_J < 27.5$ could be at redshifts $z > 3$, otherwise the Lyman limit break would be redshifted through the U band. If we assume that all of the galaxies lie at $z < 3$, the minimum amplitude of the angular correlation function, $w_{\min}(\theta)$, is realized for the redshift distribution

$$\left(\frac{dN}{dz} \right)_{\min} \propto \frac{1}{g(z)}, \quad (z < 3). \quad (6)$$

The first line of Table 2 gives the value of $w_{\min}(30'')$ for three

cosmologies, an Einstein-de Sitter model ($\Omega_0 = 1$), an open model with $\Omega_0 = 0$, and a spatially flat, low-density model with $\Omega_0 = 0.1$ and a cosmological constant $\lambda = \Lambda_0/3H_0^2 = 0.9$. The second line in Table 2 lists the median redshift \bar{z}_{\min} of the redshift distribution $(dN/dz)_{\min}$ which minimizes the amplitude of $w(\theta)$. The correlation strength that we measure from our B_J sample of faint galaxies is inconsistent with the idea that they are the high-redshift counterparts of present-day bright galaxies in an $\Omega_0 = 1$ universe if $\epsilon = -1.2$. If $\epsilon = 0$, the predicted amplitude of the $\Omega_0 = 1$ models is only marginally consistent (at about the 5% level) with our observations if the redshift distribution is close to the minimizing form $(dN/dz)_{\min}$. Low density models with $\epsilon = 0$ and the minimizing redshift distribution are compatible with our clustering constraints. Table 2 lists results for two more realistic models for dN/dz ,

$$\frac{dN}{dz} \propto z^2 \exp \left[- \left(\frac{z}{z_0} \right)^\beta \right], \quad (7)$$

which do not have sharp cutoffs at high z . Model A ($z_0 = 3$, $\beta = 9$) just satisfies the U band Lyman limit constraints on the fraction of galaxies at $z > 3$, while Model B ($z_0 = 1.8$, $\beta = 4$) places the galaxies at lower redshifts and is perhaps a more reasonable model for dN/dz (Guiderdoni & Rocca-Volmerange 1990; Koo 1986). These two models lie above our measured amplitude for $w(\theta)$ (by at least 3σ) if $\Omega = 1$ but are compatible with our observations if the universe has a low density and $\epsilon \sim 0$.

4. IMPLICATIONS

The results of the preceding sections have the following interpretations: (1) the geometry of the universe corresponds to an open Friedmann-Robertson-Walker model or a nonzero Λ model and the clustering pattern evolves strongly ($\epsilon \approx 0$). (2) The clustering evolves more rapidly than we have assumed ($\epsilon > 0$). (3) Most of the faint galaxies at $B_J \sim 26$ belong to a population that is weakly clustered and intrinsically faint at the present epoch.

The last of these explanations appears to us to be the most plausible. Our model predictions assume a spatial correlation function with correlation length $r_0 = 5.5h^{-1}$ Mpc as measured for luminous galaxies in nearby samples (Davis & Peebles 1983). However, the clustering properties of intrinsically faint galaxies are poorly determined and there is some evidence that they are clustered more weakly than luminous galaxies (see, e.g., Haynes & Giovanelli 1988; Weinberg et al. 1991). The weak clustering that we observe may thus imply that the faint galaxies at $B_J \sim 26$ are the progenitors of galaxies that are intrinsically faint at the present day.

Several authors have noted that the high surface density of faint galaxies implies a space density that is much higher than the local density of luminous galaxies if $\Lambda = 0$ (Koo 1991; Lilly

TABLE 2
MODEL PREDICTIONS FOR THE ANGULAR CORRELATION

MODEL PARAMETER	$\Omega_0 = 0, \lambda = 0$		$\Omega_0 = 1, \lambda = 0$		$\Omega_0 = 0.1, \lambda = 0.9$	
	$\epsilon = 0$	$\epsilon = -1.2$	$\epsilon = 0$	$\epsilon = -1.2$	$\epsilon = 0$	$\epsilon = -1.2$
$w_{\min}(30'')$	0.014	0.045	0.032	0.093	0.008	0.027
\bar{z}_{\min}	2.05	1.66	1.78	1.33	2.01	1.67
$w_A(30'')$	0.014	0.056	0.037	0.17	0.008	0.033
$w_B(30'')$	0.025	0.070	0.050	0.16	0.014	0.039

et al. 1991). This problem has led some authors to question whether galaxy numbers are conserved at high redshift (White 1989; Cowie & Lilly 1991; Koo 1991). The discrepancies between our $\Omega = 1$ models and the observed $w(\theta)$ may be difficult to explain if the objects at $B_J \sim 26$ are simply sub-units which merged together to form present day luminous galaxies. If this were the case, we would expect that on scales $\sim 100h^{-1}$ kpc (corresponding to an angular scale of $\sim 30''$ at $z \sim 1-3$) their clustering should be described by equation (5b) with $r_0 \approx 5.5h^{-1}$ Mpc (i.e., an evolved form of the spatial correlation function for present-day luminous galaxies). However, the high surface density of galaxies could arise from a new galaxy population that dominates over normal galaxies at magnitudes fainter than $B_J \sim 23$ (Cowie & Lilly 1991). Our results would be compatible with an $\Omega = 1$ universe if this new population is weakly clustered.

Some of the problems discussed in the previous paragraph can be avoided in cosmological models with a nonzero cosmological constant. Fukugita et al. (1990) have shown that the faint counts can be explained with plausible assumptions about galaxy evolution in models with $\Omega_0 \sim 0.1$ and $\lambda \sim 0.9$. As Table 2 shows, the amplitude of the angular correlation function in such models can be compatible with our observations of weak clustering, provided the faint galaxies are located at redshifts $z > 1$ and the clustering evolves with $\epsilon \sim 0$. Models with $\Omega_0 + \lambda = 1$ are compatible with the inflationary model of

the early universe (Peebles 1984) and have many other attractive features (see, e.g., Efstathiou et al. 1990; Turner 1991).

Our estimates of $w(30'')$ in our 24–26 B_J mag sample are consistent with the results of Windhorst & Neuschaefer (1991) at $g = 24.7$ (i.e., $B_J \sim 25$). These authors find that the amplitude of $w(\theta)$ rises at fainter magnitudes. However, as they point out, their sample becomes seriously incomplete at magnitudes fainter than $g = 24.5$, so it is not clear whether the rise in amplitude faintward of $g = 24.7$ is real.

Our data show a marginally significant trend from U to I , in the sense that the correlations become stronger as we select galaxies at redder wavelengths. This may suggest that the dominance of a weakly clustered population over the progenitors of normal galaxies decreases as one goes to the R and I bands. Clearly, further work is required to establish whether these trends are real. A detailed investigation of the angular correlation function of faint galaxies, using a variety of selection criteria, could prove useful in identifying the distinguishing characteristics of the weakly clustered objects, thereby allowing us to identify the predecessors of normal bright galaxies from the multitude of objects seen at faint magnitudes. After all, the ancestors of galaxies like our own must be present in these deep images of the sky.

This work has been supported in part by NSF grant AST-8802533 and NASA grant NAS 5-29225 to the IAS.

REFERENCES

- Carlberg, R. G. 1991, *ApJ*, 367, 385
 Colless, M., Ellis, R. S., Taylor, K., & Hook, R. N. 1990, *MNRAS*, 244, 408
 Cowie, L. L. 1989, in *The Epoch of Galaxy Formation*, ed. C. S. Frenk, R. S. Ellis, T. Shanks, A. F. Heavens, & J. A. Peacock (Dordrecht: Kluwer), 31
 Cowie, L. L., & Lilly, S. J. 1991, in *The Evolution of the Universe of Galaxies: The Edwin Hubble Centenary Symposium*, ed. R. G. Kron (ASP Conf. Series), in press
 Cowie, L. L., Lilly, S. J., Gardner, J., & McLean, I. S. 1988, *ApJ*, 332, L29
 Davis, M., Efstathiou, G., Frenk, C. S., & White, S. D. M. 1985, *ApJ*, 292, 371
 Davis, M., & Peebles, P. J. E. 1983, *ApJ*, 267, 465
 Efstathiou, G., Sutherland, W. J., & Maddox, S. J. 1990, *Nature* 348, 705
 Fukugita, M., Takahara, F., Yamashita, K., & Yoshii, Y. 1990, *ApJ*, 361, L1
 Groth, E. J., & Peebles, P. J. E. 1977, *ApJ*, 217, 385
 Guhathakurta, P., Tyson, J. A., & Majewski, S. R. 1990, *ApJ*, 357, L9
 Guiderdoni, B., & Rocca-Volmerange, B. 1990, *A&A*, 227, 362
 Haynes, M. P., & Giovanelli, R. 1988 in *Large-Scale Motions in the Universe*, ed. V. C. Rubin & G. V. Coyne (Princeton: Princeton Univ. Press), 31
 Jarvis, J. F., & Tyson, J. A. 1981, *AJ*, 86, 476
 Koo, D. C. 1986, in *Spectral Evolution of Galaxies*, ed. C. Chiosi & A. Renzini (Dordrecht: Reidel), 419
 Koo, D. C. 1991, in *The Evolution of the Universe of Galaxies: The Edwin Hubble Centenary Symposium*, ed. R. G. Kron (ASP Conf. Series), in press
 Lilly, S. J., Cowie, L. L., & Gardner, J. P. 1991, *ApJ*, 369, 79
 Neuschaefer, L. W., Windhorst, R. A., & Dressler, A. 1992, *ApJ*, in press
 Peebles, P. J. E. 1980, *The Large-Scale Structure of the Universe* (Princeton: Princeton Univ. Press)
 ———. 1984, *ApJ*, 284, 439
 Turner, M. S. 1991, *Physica Scripta*, in press
 Tyson, J. A. 1988, *AJ*, 96, 1
 Tyson, J. A., & Seitzer, P. 1988, *ApJ*, 335, 552
 Valdes, F. 1982, *Proc. SPIE*, 331, 465
 Weinberg, D. H., Szomoru, A., Guhathakurta, P., & van Gorkom, J. H. 1991, *ApJ*, 372, L13
 White, S. D. M. 1989, in *The Epoch of Galaxy Formation*, ed. C. S. Frenk, R. S. Ellis, T. Shanks, A. F. Heavens, & J. A. Peacock (Dordrecht: Kluwer), 15
 Windhorst, R. A., & Neuschaefer, L. W. 1991, in *AIP Conf. Proc., After the First Three Minutes*, ed. S. S. Holt, C. L. Bennett, & V. Trimble (New York: AIP), 322